

Article

# Energy Saving through Efficient BOG Prediction and Impact of Static Boil-off-Rate in Full Containment-Type LNG Storage Tank

Mohd Shariq Khan <sup>1,†</sup>, Muhammad Abdul Qyyum <sup>2,\*</sup>, Wahid Ali <sup>3</sup>, Aref Wazwaz <sup>1</sup>, Khursheed B. Ansari <sup>4</sup> and Moonyong Lee <sup>2,\*</sup>

<sup>1</sup> Department of Chemical Engineering, College of Engineering, Dhofar University, Salalah 211, Oman; mskhan@du.edu.om (M.S.K.); arefwazwaz@hotmail.com (A.W.)

<sup>2</sup> Department of Chemical Engineering, Yeungnam University, Dae-dong 712-749, Korea

<sup>3</sup> Department of Chemical Engineering Technology, College of Applied Industrial Technology (CAIT), Jazan University, Jazan 45142, Saudi Arabia; wzali@jazanu.edu.sa

<sup>4</sup> Department of Chemical Engineering, Zakir Husain College of Engineering and Technology, Aligarh Muslim University, Aligarh 202001, India; ansarikh5@gmail.com

\* Correspondence: maqyyum@yu.ac.kr (M.A.Q.); mynlee@yu.ac.kr (M.L.)

† These authors contributed equally.

Received: 13 September 2020; Accepted: 23 October 2020; Published: 26 October 2020



**Abstract:** Boil-off gas (BOG) from a liquefied natural gas (LNG) storage tank depends on the amount of heat leakage however, its assessment often relies on the static value of the boil-off rate (BOR) suggested by the LNG tank vendors that over/under predicts BOG generation. Thus, the impact of static BOR on BOG predictions is investigated and the results suggest that BOR is a strong function of liquid level in a tank. Total heat leakage in a tank practically remains constant, nonetheless the unequal distribution of heat in vapor and liquid gives variation in BOR. Assigning the total tank heat leak to the liquid is inappropriate since a part of heat increases vapor temperature. At the lower liquid level, BOG is under-predicted and at a higher level, it is over-predicted using static BOR. Simulation results show that BOR varies from 0.012 wt% per day for an 80% tank fill to 0.12 wt% per day at 10% tank fill.

**Keywords:** natural gas; liquefaction; regasification; LNG storage tank; BOG; BOR

## 1. Introduction

The necessity of liquefied natural gas (LNG) is continuously rising to produce power sources and fulfill transportation needs around the globe. The global gas demand in 2000 was 136 bcm and since then it has increased many folds and is projected to increase by 768 bcm in 2040 [1]. The supply chain of LNG includes its static storage tanks and transportation in specially designed ships called LNG carriers. The growth of the NG (natural gas) industry is predicated on the construction of larger storage tanks to enhance energy security policy. That growth results in more cost-effective design, construction, and operating strategies for LNG tanks, with a simultaneous reduction of its carbon footprint [2]. In particular, the design of an LNG tank plays a crucial role in determining the overall economics of the LNG supply chain. According to the British Standard BS 7777 [3], one of the crucial factors in the LNG supply chain is the evaporation losses, which determines LNG safety, technical, and economic assessment [4]. LNG is stored and transported in tanks as odorless, clear, and non-toxic cryogenic liquid (i.e., boiling point  $\approx -162$  °C). LNG occupies 1/600th of the volume of NG allowing it to be economically transported to the consumer market that is normally distant from NG reserves [5]. LNG storage tanks provide much-needed security for the safekeeping of natural gas

in both liquefaction [6] and regasification terminals [7,8]. In the regasification terminal, storage tanks facilitate the continuous release of LNG to the end-users between shipments [9,10]. During storage, the heat ingress is commonly encountered because of the large temperature differences between the tank medium and the environment, which causes LNG evaporation and the generation of boil-off gas (BOG) [11]. Regardless of the mode of operation, BOG management in the regasification terminal is a continuous process that affects the plant's economy [12]. Querol et al. [13] proposed two ways to manage BOG produced in LNG import terminals, firstly by mixing LNG and BOG in a recodensor for BOG recondensation and secondly, by using a BOG-fueled gas turbine cycle combined with a Rankine cycle. However, both ways require significant capital investment and may not be feasible for small scale tanks or terminals with humble BOG production rates. Noh et al. [14] also proposed similar options of BOG management, BOG recondensation using LNG cold, and BOG fueled gas turbine cycle concluded that power generation is better than recondensation. Li and Li [15] proposed a dynamic simulation model to minimize BOG fluctuations during ship unloading, so as to avoid NG flaring and to save energy. Saleem et al. [16] gives insight using a full scale Computational Fluid Dynamics (CFD) simulation model about boiling phenomena within the tank and concluded that surface evaporation causes BOG generation and nucleate boiling is unlikely in the tank. Yuan et al. [17] employed organic rankine cycle for integrating BOG recondensation with LNG regasification and reported significant power savings.

BOG generation is mainly caused by the inevitable heat leak to the LNG storage tank, which must be removed from the tanks to maintain their integrity [16]. Despite their thick composite insulation layers (~1 m thick) [18], LNG storage tanks are not completely immune to heat leakage. The heat ingress to an LNG storage tank may occur via conduction, convection, or radiation through the floor, wall, and roof of the tank. Thus, a methodology to effectively quantify and manage BOG is required for LNG storage tanks. Depending on their applications, LNG storage tanks are designed to be of different sizes [19]. These tanks employ several means of containment (single, double, full, and membrane) [20]. Tanks are also classified depending upon the elevation from the ground level viz. in-ground type, above-ground type, and under-ground type [21]. The single containment storage tank consists of an inner cylindrical container (made of 9% nickel-steel) that is surrounded by outer insulation (i.e., perlite), while both double and full containment storage tanks consist of inner and outer tanks that can house cryogenic LNG [22]. A full containment storage tank is also capable of controlling the venting of vapor that arises from product leakage after a credible event (any event that is recognized as sufficiently likely for the system to be designed and operated to withstand) [23]. Among these different types of designs, full containment type (also called, full integrity type) tanks are regarded as the most advanced type and have been exploited in several recently completed and ongoing projects [24], in the case of above-ground tanks. To withstand extremely low cryogenic temperatures, LNG storage tanks have an inner lining made of 9% nickel-steel alloy known for its ductility at low cryogenic temperatures [18]. During storage, the inner lining of tank is subjected to extremely low/cryogenic temperatures ( $-162\text{ }^{\circ}\text{C}$ ) from the LNG, and in the event of leakage, LNG absorbs the insulation layer of the tank and affects its performance. Thus, the outer concrete layer of the tank becomes structurally compromised because of the quick drop in temperature [25]. To minimize heat leakage, the inner nickel-steel lining is padded with different layers of insulating materials such as glass wool, load-bearing rigid glass wool, sand, plywood, and expanded perlite [3]. The arrangements of the insulating layers (i.e., the difference between tank bottom, shell, and topsides) are chosen to reduce the vaporization of LNG to less than 0.05% of the total tank volume per day [26]. However, depending on the tank aspect ratio and insulation, the vaporization of LNG can vary from 0.02 wt% to 0.1 wt% of the total LNG tank content per day [27]. Furthermore, in the case of excessive evaporation (due to continual heat leak), its removal from the LNG tank is essential to maintain the storage pressure in the range of 110–250 mbarg [28] and to avoid the excessive pressure buildup within the tank. The methods minimizing the pressure of BOG and avoiding the scaping of BOG from the tanks would be highly adaptable. The approach determining LNG tank's BOG usually considers methane as a representative

gas [29], which provides ease during the design calculations of the tank. This is because the LNG is comprised of methane, ethane, propane, nitrogen, and high molecular weight hydrocarbons, hence it becomes difficult to model the multicomponent diffusion of such gases instead of assuming a single governing gas (as methane) makes the design and safety calculations much easier [30].

In this work, the thermal design parameters (insulation type and their thicknesses) required for the rigorous estimation of heat leakage into the LNG storage tank are compiled. The parameters are then used in the thermal design of an LNG storage tank that can accommodate full cargo from the world's largest known LNG carrier ( $Q_{max}$ , operated by Qatar Petroleum) [31]. Based on the insulation parameters and size of the storage tank, a steady rate of heat leakage is calculated for different LNG levels in the storage tank. Heat leakage in the storage tank is assigned for BOG calculations, and the issue related to the tank boil-off rate (BOR) and liquid level is discussed. However, the static value of BOR used for BOG calculation over/under predicts the BOG, and the estimation is particularly erroneous when the tank is almost empty, and this issue will be discussed in Section 3.2. The tank design considerations and parameters used for thermal design are discussed in Section 2.1. Based on the acquired information, a thermal design for a 260,000 m<sup>3</sup> tank including materials of construction and the thickness of different insulating layers considering their thermal properties, is proposed. The impact of the static BOR on BOG is highlighted. The current work is regarded as part 1 for designing full containment type LNG storage tanks.

## 2. Methodology

### 2.1. LNG Tank Heat Leakage

The size of an LNG storage tank depends on the end application. In the case of city gas storage, LNG tanks are designed onshore with very large sizes [32]. So far the biggest onshore tank can store about 260,000 m<sup>3</sup> [24]. Japan, the largest consumer of LNG, utilizes 76 LNG storage tanks of three different sizes, viz. small tanks (650 m<sup>3</sup> to 10,000 m<sup>3</sup>), medium-sized tanks (10,000 m<sup>3</sup> to 90,000 m<sup>3</sup>), and large tanks (100,000 m<sup>3</sup> to 200,000 m<sup>3</sup>) [33]. South Korea, the second-largest consumer of LNG, utilizes 36 LNG tanks with storage capacities ranging from 150,000 m<sup>3</sup> to 200,000 m<sup>3</sup> [32]. Depending on the location, seismic activity, operational, and environmental conditions, the LNG storage tank can also be built as environmentally-friendly in-ground and underground types, to reduce the footprints and psychological impact associated with large tanks. There are also mobile LNG transport trailers equipped with tanks ranging from 2–30 m<sup>3</sup> [34] and up to 78 m<sup>3</sup> [35]. In this report, our discussions are limited to the thermal design aspects for a 260,000 m<sup>3</sup> full containment or full integrity type LNG storage tank. This is by far the largest proposed tank size [24] that can accommodate full cargo from the largest LNG carrier Q-Max, operated by Qatar LNG [36]. A schematic diagram of the LNG storage tank is illustrated in Figure 1.

#### 2.1.1. Insulation Properties Needed for Heat Leak Calculations

The selection of effective insulation materials for cryogenic applications is essential for safe storage operations. Insulation protects the refrigerated product from thermal vibrations and reduces heat leakage and/or ingress due to seasonal and daily ambient temperature cycles. Any damage to the insulation system can compromise product quality and safety of the regasification operation. The safe and economical operation, minimal heat leakage, and the prevention of condensation to minimize corrosion are key requirements of cryogenic insulation materials. A composite layer of insulation is applied around the inner nickel-steel core of the LNG storage tank. The density and specific heat values supplied by common insulation materials utilized in LNG tanks are compiled in Table 1.

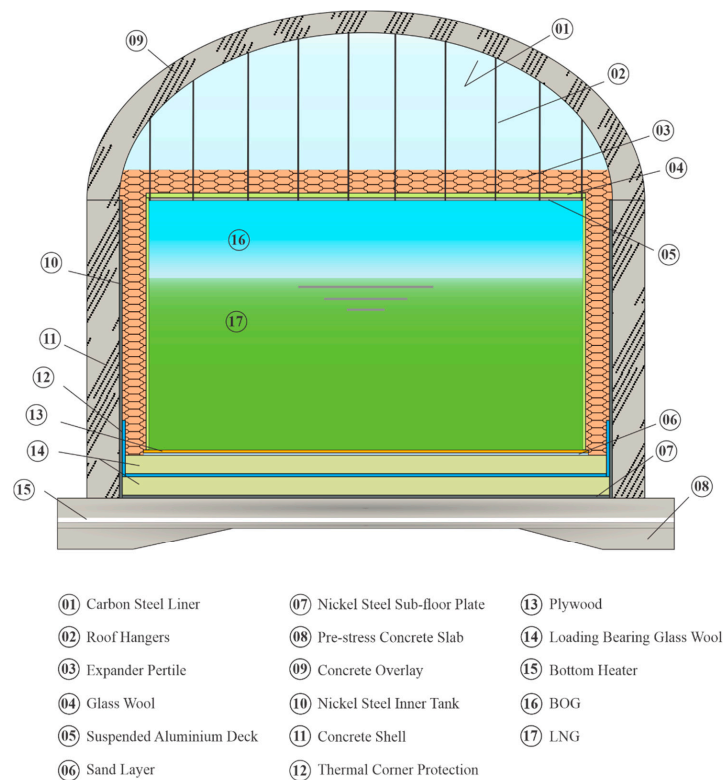


**Figure 1.** The thermal design of the liquefied natural gas (LNG) storage tank that is considered in the present work.

**Table 1.** Density and specific heat capacity of the insulation materials used in heat leakage calculations.

Insulating Material	Density (kg/m <sup>3</sup> )	Specific Heat (kJ/kgK)
Perlite (expanded)	30–150 [37]	0.837 [38]
Concrete	2400	0.960
Glass wool	24	0.670
Total Insulation	1331.7	0.783
Ni-Steel	7801	0.456

Thermal insulation properties at a mean temperature of 24 °C.

### 2.1.2. Tank Shell Heat Leakage

The shell of a full containment type LNG storage tank consists of a meter-thick concrete outer layer that protects the inner steel tank. A thick insulation layer made of expanded perlite and glass wool is sandwiched between the concrete and nickel-steel tank. The concrete outer tank is made up of a bottom slab, a pre-stressed wall, and a reinforced concrete roof. The inner tank is made of 9% nickel-steel alloy, which increases the ultimate strength, elastic limit, toughness, and retards grain growth, thereby enhancing the strength and ductility for application at cryogenic temperatures. The glass wool is typically composed of sand and 80% recycled glass and is placed adjacent to the nickel-steel tank, followed by expanded perlite. Apart from providing thermal insulation for convective heat transfer, the thin glass wool layer also provides an extra shield against radiative heat transfer. Perlite occurs naturally and is mostly silicon dioxide with approximately 6% water content. Its natural density is 1100–2000 kg/m<sup>3</sup>. When crushed and heated over 871 °C, water evaporates, and it expands by a factor of 4 to 20 times into the cells of glassy particles (called evacuated or expanded perlite) in the density range of 40–140 kg/m<sup>3</sup> [37]. This expanded perlite has low thermal conductivity and does not shrink, swell, warp, or rot. It does not retain moisture and satisfies the requirements

of fire regulations [39]. Hence, it is utilized as a major insulating material for LNG storage tanks. The pore space between the insulation is filled with BOG vapor to further decrease thermal conductivity. Further reduction in thermal conductivity is achieved by filling the pore space with argon instead of methane [39]. The typical values for the thickness and thermal properties of the materials used in the shell design of a full containment type LNG storage tank are compiled in Table 2. Both concrete and perlite have comparable thicknesses, but the thermal resistance (calculated by the usual resistance in the series model) of perlite is approximately 3 times higher than that of concrete. Therefore, the former facilitates the control of the thermal resistance on the shell side. As such, the effective total resistance of the vapor and liquid parts of the tank are only marginally different, although the resistance associated with the vapor film is nearly 100 times higher than that of the liquid film. The thermal resistance due to the air film outside the tank also depends on the wind speed and flow distribution, and a representative value is reported in Table 2. Given that the perlite layer offers the controlling resistance, the precise value of the resistance due to external air films, such as the internal vapor and liquid films, has little effect on the overall wall heat transfer resistance, and is consequently ignored in this study.

**Table 2.** Elements of LNG tank shell design.

Elements of Shell	Thickness (m)	Thermal Conductivity (W/mK)	Thermal Resistance (m <sup>2</sup> k/W)
Nickel steel tank	0.020	18.300	0.001
Glass fiber	0.150	0.050	3
Perlite (@ −126 °C) [40]	0.900	0.027	33.333
Concrete overlay	1	0.100	10
Internal vapor resistance	–	–	0.333
Outside air resistance	–	–	0.476
Shell vapor side total resistance	–	–	47.144
HTC of tank vapor side (W/m <sup>2</sup> K)	–	–	0.021
Internal to Liquid resistance	–	–	0.003
Shell liquid side total resistance	–	–	46.814
HTC of tank liquid side (W/m <sup>2</sup> K)	–	–	0.021

HTC—Heat Transfer Coefficient.

### 2.1.3. Tank Roof Heat Leakage

The full containment type tank has a steel-lined concrete hemispherical dome with a suspended ceiling deck. The steel roof liner is a 5 mm-thick steel membrane that is stiffened with rafters in radial and tangential directions, to act as a framework for the concrete overlay [32]. In certain designs, the suspended aluminum ceiling is used to hang the upper glass wool insulation material [41]. In other designs, the space between the nickel steel tank and suspended ceiling is filled with perlite and glass wool insulation. Regardless of the insulation placement, an air cavity is provided in the dome that provides further resistance to heat transfer from the tank roof side. The thermal conductivity values of the material used for a typical tank roof and the contribution of their total resistance to heat transfer from the roof side are detailed in Table 3.

**Table 3.** Elements of the LNG tank roof design.

Elements of Roof	Thickness (m)	Thermal Conductivity (W/m K)	Thermal Resistance (m <sup>2</sup> k/W)
Tank vapor side	–	–	0.333
Nickel steel tank	0.020	18.3	0.001
Suspended aluminium	0.003	205	$1.461 \times 10^{-5}$
Glass fiber	0.150	0.050	3
Perlite	0.900	0.027	33.333
Air cavity	–	–	3
Steel liner	0.005	54	$9.250 \times 10^{-5}$
Concrete overlay (8 inches)	0.203	0.1	2.032
Internal to vapor resistance	–	–	0.333
Outside to air resistance	–	–	0.476
Roof side total resistance	–	–	42.175
HTC of the tank roof (W/m <sup>2</sup> K)	–	–	0.023

#### 2.1.4. Tank Bottom Heat Leakage

The thermal and mechanical design of the bottom of an LNG storage tank takes the full product load and frost heave into consideration. Insulating material at the bottom of the tank should have a load-bearing capacity and appropriate thermal characteristics, which can be satisfied using rigid cellular-type insulation and have been applied in several designs. In some designs, a thin layer of plywood and sand is placed between the nickel-steel tank and the main insulation to enhance the thermal resistance [42]. Contraction of concrete at the storage tank base causes frost heave (i.e., upward swelling of the ground beneath the tank) that may compromise tank security. Thus, a parallel electric coil or brine-based heating system is used at the bottom concrete slab to prevent freezing of the ground. To provide mechanical strength against full tank load and liquid tightness at cryogenic temperatures, the concrete at the tank's bottom is pre-stressed by applying a permanent compressive force to the steel tendons placed in the concrete base. It is a safe practice to design a secondary bottom container and a steel liner for bottom protection in the LNG storage tank, so as to keep the LNG from seeping into the concrete and the insulation layers in the event of the failure of the first tank. The second sub-floor plate is followed by the insulation and carbon steel liner, with a thermal corner protection layer that extends 5 m above the bottom slab and protects the wall-to-base joint [42]. The typical thicknesses and contributions of the tank bottom insulation and construction materials to the total thermal resistance are given in Table 4.

**Table 4.** Elements of LNG tank bottom design.

Elements of Roof	Thickness (m)	Thermal Conductivity (W/m <sup>2</sup> K)	Thermal Resistance (m <sup>2</sup> K/W)
Internal to Liquid resistance	–	–	0.003
Nickel Steel	0.020	18.300	0.001
plywood	0.012	0.130	0.092
Sand layer	0.005	0.150	0.033
Load bearing rigid cellular glass fiber	0.500	0.040	12.500
Nickel Steel subfloor plate	0.020	18.300	0.001
Load bearing rigid cellular glass fiber	0.500	0.040	12.50
Carbon steel liner	0.001	54	$1.852 \times 10^{-5}$
Concrete slab heater	2	0.100	20
Total resistance	–	–	45.131
HTC of the tank roof (W/m <sup>2</sup> K)	–	–	0.022

## 2.2. LNG Regasification Terminal Model

The information collected through Tables 1–5 is utilized for modeling heat leakage in the tank that in turn is used for BOG and BOR predictions. An LNG storage tank operating in a regasification terminal is selected for heat modeling. The terminal is operating in holding mode where no transfer of LNG takes place to and from the carrier ship, however a small recirculation of LNG to keep the transfer line cool and a fixed continuous send out of LNG is maintained from the tank. A schematic of the LNG regasification terminal is given in Figure 2.

**Table 5.** Total thermal resistance and heat transfer coefficient value needed for heat leak calculations obtained using the values given in Tables 1–4.

Elements	Thermal Resistance ( $m^2K/W$ )		
	Roof	Shell Vap	Shell Liq
Total resistance	42.173	47.141	46.811
Heat transfer coefficient ( $W/m^2 K$ )	0.02371	0.02121	0.02136

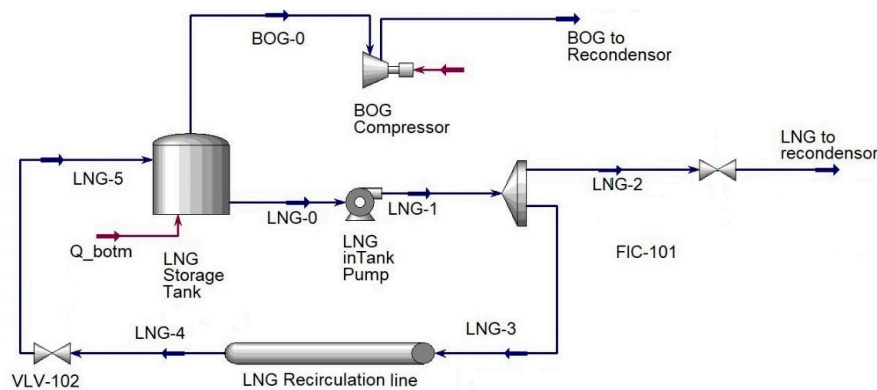


**Figure 2.** LNG regasification terminal process model considered for Boil-off gas (BOG) estimation.

### 2.2.1. Simulation Basis & Modeling Assumptions

The tank dimensions and other parameters required for heat leakage calculation are summarized in Table 6. The key assumptions used for heat leakage calculations are as follows:

- The temperature across the tank wall and insulation is assumed to be constant;
- The temperature does not vary with the height of the tank;
- Heat ingress due to the convection/conduction effect of solar radiation is ignored;
- Liquid (LNG) and vapor (BOG) phases are assumed to be well mixed (no stratification);
- Mass and heat transfer occur between holdup (LNG/BOG) phases.

Based on these assumptions and the selected parameters (Table 6) the steady rate of heat leakage is calculated from the model (Figure 2). It is worthwhile to mention now that BOG from the LNG tank is contributed by heat ingress into the tank and the recirculation lines, as well as the in-tank pump duty incurred due to recirculation. For a fixed recirculation rate a small and continuous amount of heat is added to the tank which can be ignored in comparison with tank heat leakage, and the heat generated by the in-tank pump is taken away from the tank by sending out LNG [43]. Thus, the main factor contributing to the BOG generation from the tank is ambient heat leak. The Aspen Hysys tank module along with some theoretical adjustments reported by Khan et al. [7] is utilized for heat leak modeling. The correctness of the model is validated by Effendy et al. [11].

**Table 6.** LNG storage tank model parameters and simulation basis.

Tank Dimensions and Heat Transfer Parameters	Values	Units
Volume	260,000	m <sup>3</sup>
Diameter	90	m
Height	41	m
Top side HTC	0.02371	W/m <sup>2</sup> -K
Shell vapour side HTC	0.02121	W/m <sup>2</sup> -K
Shell liquid side HTC	0.02136	W/m <sup>2</sup> -K
Vapor-liquid Interface HTC	4.00000	W/m <sup>2</sup> -K
Tank bottom temperature maintained @	5	°C
Ambient Temperature	25	°C
Tank pressure	1.17	bar
LNG density	455.5	kg/m <sup>3</sup>
Latent heat of vaporization of LNG ( $\lambda$ )	510	kJ/kg
LNG Composition		
Methane	0.9984	mole fraction
Nitrogen	0.0015	mole fraction

### 2.2.2. Tank Boil-Off-Rate (BOR)

Boil-off rate (BOR) is defined as the amount of LNG vaporization of the total LNG mass per day and given by Equation (1):

$$BOR = \frac{BOG_{Q_{liq}} \times 24}{Total\_LNG\_mass}. \quad (1)$$

BOG obtained from the (Aspen Hysys tank module using all the parameters given in Tables 1–5) the heat leak to the liquid ( $BOG_{Q_{liq}}$ ) is plugged in Equation (1) to obtain BOR. A problem in the definition of BOR is that it considers the worst case of heat leakage for BOG calculations [20]. The worst case is a situation involving heat leakage in a tank with a very low liquid level. However, the tank operates from high to low liquid level and is not always at a low level. This makes BOR a function of liquid level in the tank. This issue is discussed in Section 3.1 by considering the three cases of 80%, 50%, and 10% liquid level in the tank.

## 3. Results and Discussion

### 3.1. BOR Variation with Tank Liquid Level

To calculate the heat leakage in an LNG storage tank, the liquid-vapor contact area (depending on the LNG level), ambient temperature, and heat transfer coefficient (HTC) values are required. Considering a constant ambient temperature (which is approximately true for tropical climates), only the level of LNG in the storage tank is a variable. Thus, the effect of different LNG levels on heat ingress is considered. The scenarios of 80%, 50%, and 10% of the LNG volume in the storage tank are considered during heat leakage calculation. The details of this process are summarized in Table 6.

#### 3.1.1. LNG Tank 80% Occupied by Liquid

For the 80% tank fill, the vapor and liquid are assumed to be in equilibrium. This assumption is reasonable because when the storage tank is filled with fresh LNG, the hot vapor (if already present in the tank) is displaced by the cold LNG, leaving a small vapor space that is eventually filled by BOG, in equilibrium with LNG. The total steady heat leakage for a tank filled at 80% is approximately 100 kW, for which the liquid receives 62 kW and the remainder is due to the vapor space (roof 28% and the side vapor 10%). If all the heat leakage is assigned to the BOG generation, it is over-predicted by 37%. Hence, it is not appropriate to assign all the heat leakage into the tank to BOG generation, although this is a common practice in several studies [44]. For an 80% LNG fill in the tank, the boil-off



rate BOR (% of liquid vaporization of the total liquid volume per day) is 0.01%, which is within the safe limit (i.e., 0.05%) stated in the literature [26].

### 3.1.2. LNG Tank 50% Occupied by Liquid

A tank volume 50% filled with LNG provides more vapor area for heat transfer compared to 80% filling. This increase in the vapor area increases its temperature to  $-145\text{ }^{\circ}\text{C}$  [11] by more heat transfer. The rise of the vapor temperature is attributed to the higher heat capacity of LNG, and the significant temperature difference between BOG/LNG ( $\approx 13.5\text{ }^{\circ}\text{C}$ ) [44] causes 89% of the heat leakage in the vapor phase to be transferred to the LNG via the vapor-liquid interface. The heat loss through interface increases only by 1% for the 10% LNG filled scenario (cf. Table 7). This is because the vapor temperature is no longer increasing when the tank is emptied from 80% to 50%. After saturation in the increase of the vapor temperature, any heat leakage to the vapor is simply transferred to the LNG. In the case of 50% tank filling, if all the heat leakage from the roof and shell vapor side is assigned to the liquid, the BOG generation is over-predicted by 5.5%. Thus, in this case, the overprediction is significantly smaller compared to the 80% tank fill scenario, due to the vapor-liquid interface heat transfer phenomenon, which is absent when the vapor and liquid temperatures are equal. At this rate of heat transfer, the BOR from the tank is approximately 0.03%, which is within the limit outlined in the International Gas Union 2011 annual report [27].

**Table 7.** The steady rate of heat leakage in the LNG tank for different liquid levels.

Elements of Heat Leak Calculations	Tank 80% Fill	Tank 50% Fill	Tank 10% Fill
Heat leak from tank roof (kW)	27.74	25.64	24.88
Heat leak from tank bottom (kW)	25.91	25.79	25.86
Heat leak from tank vapor area (kW)	9.04	20.89	36.51
Heat leak from tank liquid area (kW)	36.65	22.72	4.53
Heat leak from vapor to liquid (kW)	0.0	41.27	55.03
Liquid level in the tank (h) (m)	32.8	20.50	4.10
Shell side liquid contact area ( $\text{m}^2$ )	9326.2	5796.2	1159.2
Shell side vapor contact area ( $\text{m}^2$ )	2317.3	5796.2	10,433.2
Liquid temperature ( $^{\circ}\text{C}$ )	$-159$	$-158.5$	$-158$
Vapor Temperature ( $^{\circ}\text{C}$ ) [11]	$-159$	$-145$	$-140$
Total ambient heat leak to the tank (kW)	99.34	95.11	91.78
Total ambient heat leak to liquid (kW)	62.56	89.85	85.42
BOG rate (with roof & vapor heat to liquid) (kg/h)	701	671.4	647.9
BOG rate (with actual heat leak) (kg/h)	441.6	634.2	602.9
Boil-off rate (BOR) (wt%)	0.012	0.026	0.12

### 3.1.3. LNG Tank 10% Occupied by Liquid

For 10% tank filling, the vapor temperature further increases to  $-140\text{ }^{\circ}\text{C}$  ( $-145\text{ }^{\circ}\text{C}$  for 50% tank filling) [11]. In this case, the steady heat leak calculation predicts a BOR of 0.12%, which is much higher when compared to the previous two cases (of 80% and 50% tank fillings). This is because of a small amount of liquid LNG in the tank. At the 10% LNG level, all heat leakage to the vapor is transferred to the LNG. The heat capacity of the LNG is much smaller for the 10% liquid level therefore, any heat leakage simply boils the LNG to a much higher BOG rate.

It is worthwhile to note that the total amount of heat leakage into the tank decreases by only 8% for a fill level from 80% to 10% (see Figure 3). This reduction in heat leakage is not significant and can be assumed to be negligible for practical applications. Interestingly, the BOG generation is found to increase significantly by 27% (cf. Figure 4). A similar trend in BOR (increment of 90%, i.e., from 0.012 wt% to 0.12 wt% per day) is observed (cf. Figure 5). The sharp rise in BOR is attributed to the receding liquid level in the tank, which leads to the depletion of the liquid's heat capacity.

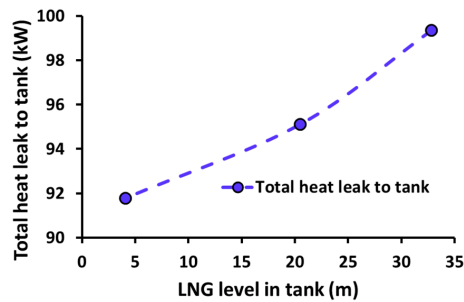


Figure 3. Total heat leakage to the tank.

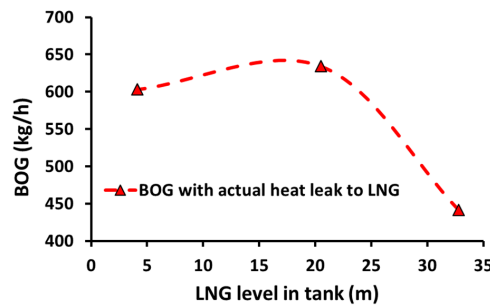


Figure 4. BOG with actual heat leakage to LNG.

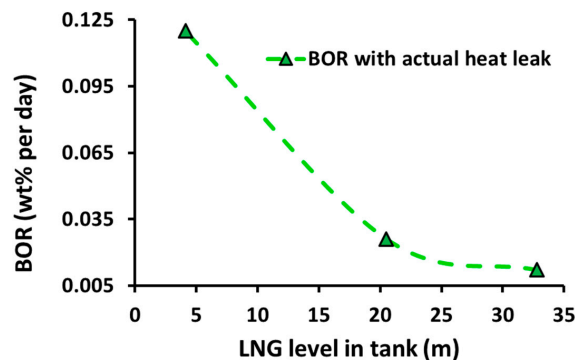


Figure 5. BOR with actual heat leakage to LNG.

### 3.2. Impact of Static BOR on BOG Predictions

BOR (wt%) corresponds to the LNG vaporized per day of the total LNG mass present in the tank. Most often, the designer uses a fixed value of 0.05 wt% (on the gross volume of the LNG inner tank and pure methane) for the maximum tank volume as the BOG generation rate. This number is only reliable when the total amount of heat leakage into the tank is constant, irrespective of the actual LNG volume inside the tank, as evident from Figure 3 (i.e., 8% increase of the total heat ingress in the tank, and confirms that the heat leakage in the tank is practically constant). However, this definition assigns all the heat leakage of the tank to the liquid phase and ignores the distribution of the heat into the vapor and liquid, and the effect of change of the liquid level on the BOR and BOG, which is addressed in this section.

If all the heat leakage of the tank is assigned to the liquid, the BOG over prediction is significant at a higher liquid level, as shown in Figure 4. This is because of the high heat ingress in the vapor, as discussed in Section 3.1.1 for an 80% filled tank. BOG production in an LNG storage tank is often determined using the vendor-supplied static BOR value. In the present work, it has been established that BOR is not static (although the total heat ingress in the tank is practically constant) and strongly depends on the liquid level in the tank (see Figure 6). Using static BOR for the design of LNG tank upstream units such as compressors and recondensers may cause serious issues in BOG handling. Thus, for a practical design, appropriate provisions must be made to address BOG based on worst case

BOR. BOG is often calculated by assigning all heat ingress to the liquid, ignoring the effect of heat distribution in vapor and liquid. This approach may lead to the wrong estimation of both BOG and BOR (see Figure 7).

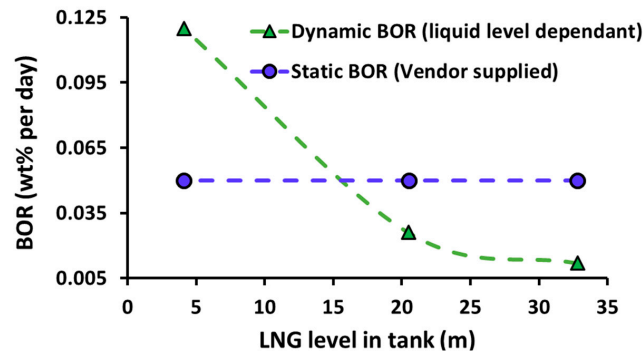


Figure 6. Static vs dynamic BOR in the tank.

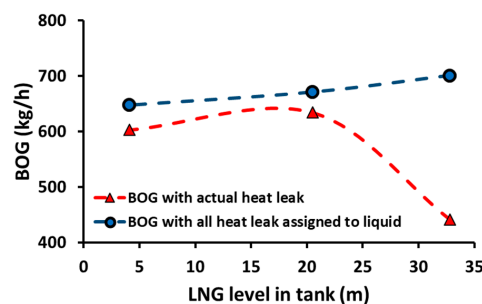


Figure 7. BOG over prediction with heat leak.

### 3.3. Limitations and Unique Findings

The thermal design of LNG storage tanks and the impact of static BOR on BOG is presented. The expanded perlite and concrete facilitate the control of resistance of approximately 70% and 21% for the LNG tank shell, respectively. For the roof design, 70% resistance is provided by perlite, while the remainder is compensated for by the glass wool, air cavity, and concrete overlay. Based on the considered thermal design parameters, the rate of heat leakage from the tank's roof, shell, and the bottom is calculated for different LNG filling levels of the storage tank. The heat leakage is then used to estimate the tank's BOR. It was determined that the heat leakage in the tank remains practically constant however, the distribution of heat in the vapor and liquid varies. This variation changes the BOR in the tank.

#### 3.3.1. Study Limitations

The thermal design presented in the current work can serve as a good starting point for rigorous heat leakage design in LNG storage tanks. LNG tank operation is inherently dynamic thus, the assumptions made in this work for the steady-rate of heat leakage can hold for a tank with LNG stored for a sufficiently long time at different liquid levels. If appropriate estimates of the tank vapor and liquid temperature are available, the steady rate heat leakage model can be used for any tank otherwise, a fully dynamic model of LNG tank operation must be made to calculate the boil-off gas. The following observations were made based on the study that can assist in assessing BOG generation from the LNG storage tank.

#### 3.3.2. Unique Findings

The following unique finding was made through the study that can help in assessing correct BOG at a different liquid level:

- Total heat leakage in the LNG tank is essentially constant;
- Assigning that all the tank heat leakage to the liquid is inappropriate;
- Some part of the vapor heat leak increases its temperature;
- BOR strongly depends on the tank liquid level;
- The distribution of heat in the vapor and liquid changes the BOR;
- At a low liquid level, the BOG is under-predicted using static BOR;
- At a high liquid level, the BOG is over-predicted using static BOR;
- BOG predictions must be based on heat leakage rather than static BOR;
- Vapor to liquid heat transfer plays a significant role in BOR predictions.

**Author Contributions:** Conceptualization, M.S.K., and M.A.Q.; methodology, M.S.K., and M.A.Q.; software, W.A.; formal analysis, W.A. and K.B.A.; investigation, M.S.K., and M.A.Q.; writing—original draft preparation, M.S.K.; writing—review and editing, M.S.K., M.A.Q., A.W., and K.B.A.; visualization, A.W.; supervision, M.L.; All authors have read and agreed to the published version of the manuscript.

**Funding:** This research was funded by TRC OMAN, block funding grant number BFP/RGP/EI/18/152 & BFP/RGP/EI/19/197. This work was also supported by the Priority Research Centers Program through the National Research Foundation (NRF) of Korea funded by the Ministry of Education (2014R1A6A1031189).

**Acknowledgments:** The authors are grateful to Laura Savoldi (head of MAHTEP Group, Dipartimento Energia “Galileo Ferraris”, Politecnico di Torino, Corso Duca degli Abruzzi 24, 10129 Torino, Italy) for useful discussions and suggestions to improve the quality of the manuscript.

**Conflicts of Interest:** The authors declare no conflict of interest.

## References

1. IEA. *World Energy Outlook 2019—Analysis-IEA*; International Energy Agency: Paris, France, 2019.
2. Migliore, C.; Salehi, A.; Vesovic, V. A non-equilibrium approach to modelling the weathering of stored Liquefied Natural Gas (LNG). *Energy* **2017**. [[CrossRef](#)]
3. BSI. *Flat-Bottomed, Vertical, Cylindrical Storage Tanks for Low Temperature Service Part 2: Specification for the Design and Construction of Single, Double and Full Containment Metal Tanks for the Storage of Liquefied Gas at Temperatures down to −165 Degrees*; BSI: London, UK, 1993.
4. Hasan, M.M.F.; Zheng, A.M.; Karimi, I.A. Minimizing boil-off losses in liquefied natural gas transportation. *Ind. Eng. Chem. Res.* **2009**, *48*, 9571–9580. [[CrossRef](#)]
5. Khan, M.S.; Lee, M. *Optimization of Natural Gas Liquefaction Process*; IGI Global: Hershey, PA, USA, 2015; ISBN 9781466683990.
6. Khan, M.S.; Lee, S.; Rangaiah, G.P.; Lee, M. Knowledge based decision making method for the selection of mixed refrigerant systems for energy efficient LNG processes. *Appl. Energy* **2013**. [[CrossRef](#)]
7. Khan, M.S.; Effendy, S.; Karimi, I.A.; Wazwaz, A. Improving design and operation at LNG regasification terminals through a corrected storage tank model. *Appl. Therm. Eng.* **2019**. [[CrossRef](#)]
8. Lee, I.; Park, J.; Moon, I. Conceptual design and exergy analysis of combined cryogenic energy storage and LNG regasification processes: Cold and power integration. *Energy* **2017**, *140*, 106–115. [[CrossRef](#)]
9. Lee, I.; Park, J.; You, F.; Moon, I. A novel cryogenic energy storage system with LNG direct expansion regasification: Design, energy optimization, and exergy analysis. *Energy* **2019**. [[CrossRef](#)]
10. Rao, H.N.; Karimi, I.A. Optimal design of boil-off gas reliquefaction process in LNG regasification terminals. *Comput. Chem. Eng.* **2018**, *117*, 171–190.
11. Effendy, S.; Khan, M.S.; Farooq, S.; Karimi, I.A. Dynamic modelling and optimization of an LNG storage tank in a regasification terminal with semi-analytical solutions for N<sub>2</sub>-free LNG. *Comput. Chem. Eng.* **2017**. [[CrossRef](#)]
12. Kurle, Y.M.; Wang, S.; Xu, Q. Simulation study on boil-off gas minimization and recovery strategies at LNG exporting terminals. *Appl. Energy* **2015**, *156*, 628–641. [[CrossRef](#)]
13. Querol, E.; Gonzalez-Regueral, B.; García-Torrent, J.; García-Martínez, M.J. Boil off gas (BOG) management in Spanish liquid natural gas (LNG) terminals. *Appl. Energy* **2010**, *87*, 3384–3392. [[CrossRef](#)]

14. Noh, Y.; Kim, J.; Kim, J.; Chang, D. Economic evaluation of BOG management systems with LNG cold energy recovery in LNG import terminals considering quantitative assessment of equipment failures. *Appl. Therm. Eng.* **2018**. [CrossRef]
15. Li, Y.; Li, Y. Dynamic optimization of the boil-off gas (BOG) fluctuations at an LNG receiving terminal. *J. Nat. Gas Sci. Eng.* **2016**, *30*, 322–330. [CrossRef]
16. Saleem, A.; Farooq, S.; Karimi, I.A.; Banerjee, R. A CFD simulation study of boiling mechanism and BOG generation in a full-scale LNG storage tank. *Comput. Chem. Eng.* **2018**. [CrossRef]
17. Yuan, T.; Song, C.; Bao, J.; Zhang, N.; Zhang, X.; He, G. Minimizing power consumption of boil off gas (BOG) recondensation process by power generation using cold energy in liquefied natural gas (LNG) regasification process. *J. Clean. Prod.* **2019**, *238*, 117949. [CrossRef]
18. Saitoh, N.; Muraoka, H.; Yamaba, R.; Saeki, O. *Development of Heavy 9% Nickel Steel Plates with Superior Low-Temperature Toughness for LNG Storage Tanks*; Nippon Steel Technical Report; Nippon Steel: Chiyoda City, Tokyo, Japan, 1993.
19. Lun, H.; Fillippone, F.; Roger, D.C.; Poser, M. Design and construction aspects of post-tensioned LNG storage tank in Europe and Australasia. In Proceedings of the New Zealand Concrete Industry Conference, Christchurch, New Zealand, 29 September–1 October 2006.
20. Thierçault, J.; Egels, C. Cryogenic above ground storage tanks: Full containment and membrane comparison of technologies. In Proceedings of the IGT International Liquefied Natural Gas Conference Proceedings, Houston, TX, USA, 6–19 April 2013.
21. Reddy Gorla, R.S. Probabilistic analysis of a liquefied natural gas storage tank. *Appl. Therm. Eng.* **2010**. [CrossRef]
22. Chamberlain, G.A. Management of large LNG hazards. In Proceedings of the International Gas Union World Gas Conference Papers, Amsterdam, The Netherlands, 5–9 June 2006.
23. GIIGNL. Information Paper No. 5-Managing LNG Risks–Containment. Available online: <http://www.giignl.org/> (accessed on 25 August 2020).
24. SLNG. *Singapore LNG Terminal*; SLNG: Alexandra Rd, Singapore, 2013.
25. Jeon, S.-J.; Jin, B.-M.; Kim, Y.-J.; Chung, C.-H. Consistent thermal analysis procedure of LNG storage tank. *Struct. Eng. Mech.* **2007**, *25*, 445–466. [CrossRef]
26. Dobrota, Đ.; Lalić, B.; Komar, I. Problem of Boil-off in LNG Supply Chain. *Trans. Marit. Sci.* **2013**. [CrossRef]
27. IGU. *World LNG Report 2011*; IGU: Barcelona, Spain, 2011.
28. Shin, Y.; Lee, Y.P. Design of a boil-off natural gas reliquefaction control system for LNG carriers. *Appl. Energy* **2009**. [CrossRef]
29. Miana, M.; del Hoyo, R.; Rodríguez, V.; Valdés, J.R.; Llorens, R. Calculation models for prediction of Liquefied Natural Gas (LNG) ageing during ship transportation. *Appl. Energy* **2010**. [CrossRef]
30. Kim, H.S.; Shin, M.W.; Yoon, E.S. Optimization of operating procedure of LNG storage facilities using rigorous BOR model. In Proceedings of the IFAC Proceedings Volumes (IFAC-PapersOnline), Seoul, Korea, 6–11 July 2008.
31. Qatargas. *The Pioneer*; Magazin of Qatargas Operating Company: Doha, Qatar, 2019; p. 34.
32. Yang, Y.M.; Kim, J.H.; Seo, H.S.; Lee, K.; Yoon, I.S. Development of the world’s largest above-ground full containment LNG storage tank. In Proceedings of the International Gas Union World Gas Conference Papers, Amsterdam, The Netherlands, 5–9 June 2006.
33. Development and Construction of Large-Capacity Full Containment LNG Tank/By Technology Classification|Technology|OSAKA GAS. Available online: [https://www.osakagas.co.jp/en/rd/technical/1198900\\_6995.html](https://www.osakagas.co.jp/en/rd/technical/1198900_6995.html) (accessed on 6 August 2020).
34. Transport Trailers -Worthington Industries. Available online: <https://worthingtonindustries.com/Products/Small-Scale-LNG/Transport-Trailers> (accessed on 6 August 2020).
35. LNG Transport|Cryolor. Available online: <https://www.cryolor.com/lng-transport> (accessed on 6 August 2020).
36. Available online: <https://www.qatargas.com/english/MediaCenter/ThePioneer/Pioneer157English.pdf> (accessed on 9 August 2020).
37. Maxim, L.D.; Niebo, R.; McConnell, E.E. Perlite toxicology and epidemiology—A review. *Inhal. Toxicol.* **2014**, *26*, 259–270. [CrossRef]
38. Perlite.org. Physical Characteristics of Perlite. Available online: <https://www.perlite.org/wp-content/uploads/2018/03/physical-characteristics-perlite.pdf> (accessed on 12 August 2020).

39. Perlite Institute, Inc. Perlite for Non-Evacuated Cryogenic and Low Temperature Service. 2013. Available online: <https://www.perlite.org/wp-content/uploads/2018/03/perlite-cryogenic-service.pdf> (accessed on 13 September 2020).
40. Gulf Perlite LLC. Available online: <https://www.gulfperlite.com/product/perlite-cryogenic-insulation> (accessed on 12 August 2020).
41. Féger, D. An innovative way of reducing bog on existing or newbuilt LNG storage tanks. In Proceedings of the IGT International Liquefied Natural Gas Conference Proceedings, Oran, Algeria, 18–21 April 2010.
42. Hoyle, K. Composite Concrete Cryogenic Tank (C3T): A Precast Concrete Alternative for LNG Storage. In Proceedings of the 17th International Conference & Exhibition on Liquefied Natural Gas (LNG 17), Houston, TX, USA, 14–19 April 2013.
43. Ebara Corporations Cryodynamics. Available online: <https://www.elliott-turbo.com/Files/Admin/Cryodynamics/submergeded-cryogenic-pumps-and-expanders-cryodynamic-products.pdf> (accessed on 8 September 2020).
44. Wordu, A.A.; Peterside, B. Estimation of Boil-off-Gas BOG from Refrigerated Vessels in Liquefied Natural Gas Plant. *Int. J. Eng. Technol.* **2013**, *3*, 44–49.

**Publisher's Note:** MDPI stays neutral with regard to jurisdictional claims in published maps and institutional affiliations.



© 2020 by the authors. Licensee MDPI, Basel, Switzerland. This article is an open access article distributed under the terms and conditions of the Creative Commons Attribution (CC BY) license (<http://creativecommons.org/licenses/by/4.0/>).